

The influence of microlensing on the shape of the AGN Fe K α line

L. Č. Popović^{1,2}, E. G. Mediavilla³, P. Jovanović^{1,2}, and J. A. Muñoz³

¹ Astronomical Observatory, Volgina 7, 11160 Belgrade 74, Serbia

² Isaac Newton Institute of Chile, Yugoslavia Branch

³ Instituto de Astrofísica de Canarias, 382005 La Laguna, Tenerife, Spain

Received 12 July 2002 / Accepted 14 November 2002

Abstract. We study the influence of gravitational microlensing on the AGN Fe K α line confirming that unexpected enhancements recently detected in the iron line of some AGNs can be produced by this effect. We use a ray tracing method to study the influence of microlensing in the emission coming from a compact accretion disc considering both geometries, Schwarzschild and Kerr.

Thanks to the small dimensions of the region producing the AGN Fe K α line, the Einstein Ring Radii associated to even very small compact objects have size comparable to the accretion disc hence producing noticeable changes in the line profiles. Asymmetrical enhancements contributing differently to the peaks or to the core of the line are produced by a microlens, off-centered with respect to the accretion disc.

In the standard configuration of microlensing by a compact object in an intervening galaxy, we found that the effects on the iron line are two orders of magnitude larger than those expected in the optical or UV emission lines. In particular, microlensing can satisfactorily explain the excess in the iron line emission found very recently in two gravitational lens systems, H 1413+117 and MG J0414+0534.

Exploring other physical scenarios for microlensing, we found that compact objects (of the order of one Solar mass) which belong to the bulge or the halo of the host galaxy can also produce significant changes in the Fe K α line profile of an AGN. However, the optical depth estimated for this type of microlensing is very small, $\tau \sim 0.001$, even in a favorable case.

Key words. galaxies: microlensing: Seyfert – line: profiles – accretion, accretion discs

1. Introduction

The influence of microlensing on the line profile of Active Galactic Nuclei (AGNs) has been discussed by several authors. On the basis of the standard model for AGNs it was accepted that the region generating the Broad Emission Lines (BELs) was too large to be affected by microlensing by a Solar mass star (Nemiroff 1988; Schneider & Wambsganss 1990). However, recent studies indicate that the BLR size is smaller than supposed in the standard model (Wandel et al. 1999; Kaspí et al. 2000). According to this, Popović et al. (2001a) considered the influence of microlensing on the spectral line profile generated by a relativistic accretion disc in the Schwarzschild geometry, finding that significant changes in the line profile can be induced by microlensing. Abajas et al. (2002) noted that this effect can be very strong for high ionization lines arising from the inner region of the accretion disc and identified a group of ten gravitational lens systems in which microlensing of emission line region could be observed. The scope of these studies has been the region where the broad UV and optical lines are generated. However, microlensing detection should be much

more favorable in a compact region generating the X-ray radiation (Popović et al. 2001b).

The X-rays of AGNs are generated in the innermost region of an accretion disc around a central super-massive Black Hole (BH). An emission line from iron K α (Fe K α) has been observed at 6–7 keV in the vast majority of AGNs (see e.g. Nandra et al. 1997; Fabian et al. 2000). This line is probably produced in the very compact region near the BH of an AGN (Iwashawa et al. 1999; Nandra et al. 1999; Fabian et al. 2000) and can bring essential information about the plasma conditions and the space geometry around the BH. Thus it seems clear that the Fe K α line can be strongly affected by microlensing and recent observations of two lens systems seem to support this idea (Oshima et al. 2001; Chartas et al. 2002).

According to this, the aim of this paper is to investigate the influence of microlensing on the AGN Fe K α line shape originated in a compact accretion disc around non-rotating and rotating BH. In Sect. 2 we discuss the construction of an accretion disc image from photons traveling in a rotating (Kerr) and non-rotating (Schwarzschild) black hole space-time geometry, including microlensing by a compact object. In Sect. 3 we analyze the consequences and signatures of gravitational microlensing. In Sect. 4 the effects of microlensing in the Fe K α line are explored in two different physical scenarios.

Send offprint requests to: L. Č. Popović,
e-mail: lpopovic@aob.bg.ac.yu

2. Observed flux from a compact accretion disc affected by microlensing

The effects of microlensing on a compact accretion disc have been previously analyzed by Popović et al. (2001b) and Chartas et al. (2002). However, these authors do not strictly include the effects of ray bending caused by the black hole that significantly distorts the image of the accretion disc. To take into account this effect, we will use the ray tracing method (Bao et al. 1994; Bromley et al. 1997; Fanton et al. 1997; Čadež et al. 1998) considering only those photon trajectories that reach the sky plane at a given observer's angle θ_{obs} . We will adopt the analytical approach proposed by Čadež et al. (1998). If X and Y are the impact parameters that describe the apparent position of each point of the accretion disc image on the celestial sphere as seen by an observer at infinity, the amplified brightness is given by

$$I_p = \varepsilon(r)g^4(X, Y)\delta(x - g(X, Y))A(X, Y), \quad (1)$$

where $x = \nu_{\text{obs}}/\nu_0$ (ν_0 and ν_{obs} are the transition and observed frequencies, respectively); $g = \nu_{\text{em}}/\nu_{\text{obs}}$ (ν_{em} is the emitted frequency from the disc), and $\varepsilon(r)$ is the emissivity in the disc, $\varepsilon(r) = \varepsilon_0 \cdot r^{-q}$. $A(X, Y)$ is the amplification caused by microlensing. We will consider two different approximations to estimate this quantity.

2.1. Microlensing by an isolated compact object

In this case the amplification is given by the relation (see e.g. Narayan & Bartelmann 1999):

$$A(X, Y) = \frac{u^2(X, Y) + 2}{u(X, Y)\sqrt{u^2(X, Y) + 4}}, \quad (2)$$

where $u(X, Y)$ corresponds to the angular separation between lens and source in Einstein Ring Radius (ERR) units and is obtained from

$$u(X, Y) = \frac{\sqrt{(X - X_0)^2 + (Y - Y_0)^2}}{\eta_0}, \quad (3)$$

X_0, Y_0 are the coordinates of the microlens with respect to the disc center (given in gravitational radii), and η_0 is the Einstein Ring Radius (ERR) expressed in gravitational radii.

The total observed flux is given by

$$F(x) = \int_{\text{image}} I_p(x) d\Omega, \quad (4)$$

where $d\Omega$ is the solid angle subtended by the disc in the observer's sky and the integral extends over the whole (line) emitting region.

2.2. Microlensing by a straight fold caustic

In most of cases we can not simply consider that microlensing is caused by an isolated compact object but we must take into account that the micro-deflector is located in an extended object (typically, the lens galaxy). In this case, when the size of the ERR of the microlens is larger than the size of the accretion

disc, we can describe the microlensing in terms of the crossing of the disc by a straight fold caustic (Schneider et al. 1992). The amplification at a point close to the caustic is given by (Chang & Refsdal 1984),

$$A(X, Y) = A_0 + \frac{K}{\sqrt{\kappa(\xi - \xi_c)}} \cdot H(\kappa(\xi - \xi_c)), \quad (5)$$

where A_0 is the amplification outside the caustic, $K = A_0\beta\sqrt{\eta_0}$ is the caustic amplification factor, where β is constant of order of unity (e.g. Witt et al. 1993). ξ is the distance perpendicular to the caustic in gravitational radii units and ξ_c is the minimum distance from the disc center to the caustic. Thus,

$$\xi_c = \sqrt{X_c^2 + Y_c^2}, \quad (6)$$

$$\text{tg}\alpha = \frac{Y_c}{X_c}, \quad (7)$$

and

$$\xi = \xi_c + \frac{(X - X_c)\text{tg}\phi + Y_c - Y}{\sqrt{\text{tg}^2\phi + 1}}, \quad (8)$$

where $\phi = \alpha + \pi/2$. $H(\kappa(\xi - \xi_c))$ is the Heaviside function, $H(\kappa(\xi - \xi_c)) = 1$, for $\kappa(\xi - \xi_c) > 0$, otherwise it is 0. κ is ± 1 , it depends on the direction of caustic motion; if the direction of the caustic motion is from approaching side of the disc $\kappa = -1$, otherwise it is $+1$. Also, in the special case of caustic crossing perpendicular to the rotating axis $\kappa = +1$ for direction of caustic motion from $-Y$ to $+Y$, otherwise it is -1 .

3. Results

To study the influence of MLE on the Fe K $_{\alpha}$ line we adopt for the disc parameters the averaged values given by Nandra et al. (1997) from the study of 18 Seyfert 1 galaxies: $i = 30^\circ$ and $q = 2.5$. For the inner radius we take $R_{\text{in}} = R_{\text{ms}}$, where R_{ms} is the radius of the marginal stability orbit, that corresponds to $R_{\text{ms}} = 6 R_g$ in the Schwarzschild metric and to $R_{\text{ms}} = 1.23 R_g$ in the case of the Kerr metric with angular momentum $a = 0.998$. Considering that for the adopted emissivity ($q = 2.5$), the emission is concentrated in the innermost part of the disc, we adopt for the outer radius $R_{\text{out}} = 20 R_g$.

3.1. Microlensing by an isolated compact object

We have computed the amplified line profile for different locations with respect to the center of the disc of a microlens of projected Einstein radius $\eta_0 = 10 R_g$. In Figs. 1 and 2 we show the results for the Schwarzschild and Kerr metrics, respectively. The distortions of the line shape remind of the ones obtained in the case of the optical disc (Popović et al. 2001a) but the effects of microlensing are stronger in the case of the X-ray disc even when we consider two order of magnitude smaller microlenses. Notice also that the inclination that we have adopted for the disc is relatively low ($i = 30^\circ$) and that for higher values of this parameter the effects will be considerably increased (see Fig. 3).

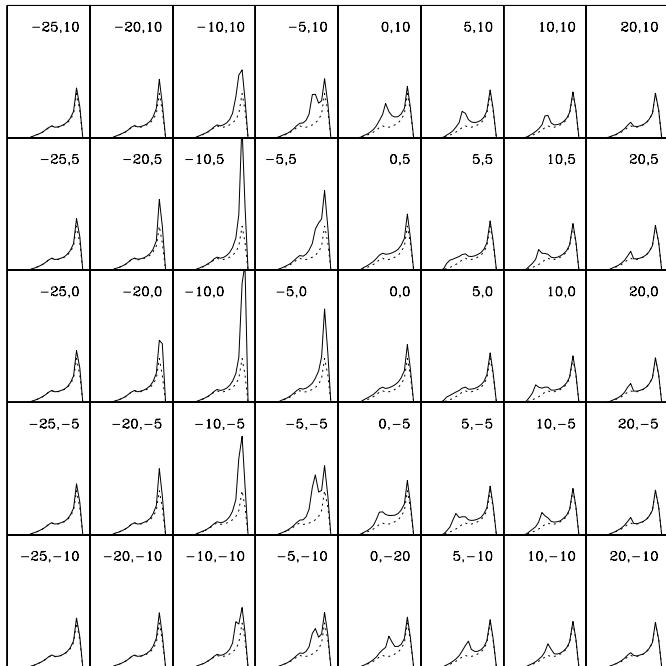


Fig. 1. The Fe K_α line profiles for different positions of the microlens. The calculations were performed for a disc in the Schwarzschild metric with parameters: $R_{\text{in}} = 6 R_g$, $R_{\text{out}} = 20 R_g$, $i = 35^\circ$, and $q = 2.5$. The ERR of the microlensing object is $10 R_g$. The relative intensity is in the range from 0 to 3, and v/v_0 is in the range from 0.4 to 1.2. The numbers at the top of the figures are the positions of the microlens (X_0 , Y_0) with respect to the disc center in gravitational radii.

Several outstanding changes of the line shape with the location of the microlens, and consequently with the transit of a microlens across the disc, can be inferred from Figs. 1 and 2. In the first place the number of peaks, their relative separation and the peak velocity could change (this also affects to the velocity centroid). In the second place, the transit of a microlens would induce an asymmetrical enhancement of the line profile. For both metrics the amplification has a maximum for negative values of X_0 that correspond to the approaching part of the rotating disc. This amplification affects mainly the blue part of the line, although the asymmetrical enhancement induced by microlensing is more blue-ward in the Schwarzschild than in the Kerr metric.

3.2. Microlensing by a straight fold caustic

In this case we have used the following parameters in Eq. (5): $A_0 = 1$, $\beta = 1$ and $\text{ERR} = 50 R_g$. We have studied the caustic crossing from different orientations finding results similar to the ones obtained in the previous section for the isolated microlens. In Figs. 4 (Schwarzschild) and 5 (Kerr) we show the changes induced in the line profile by a caustic crossing perpendicular (first two sets of lines) and along (the third and fourth sets of lines) the rotation axis starting from both sides of the disc, i.e. for $\kappa = \pm 1$ respectively. In Figs. 4 and 5 we also present the corresponding variations of line flux (below the sets of lines) for the whole line (solid line) and for the blue (v/v_0 is 0.4–0.9, dashed line, — — —), central (0.9–1.0, - - -) and red

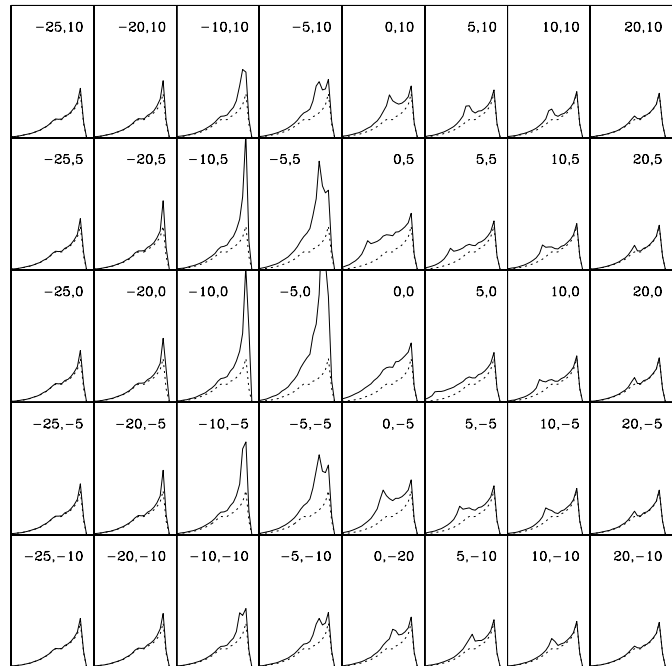


Fig. 2. The same as in Fig. 1, but for a rotating Kerr BH with $a = 0.998$.

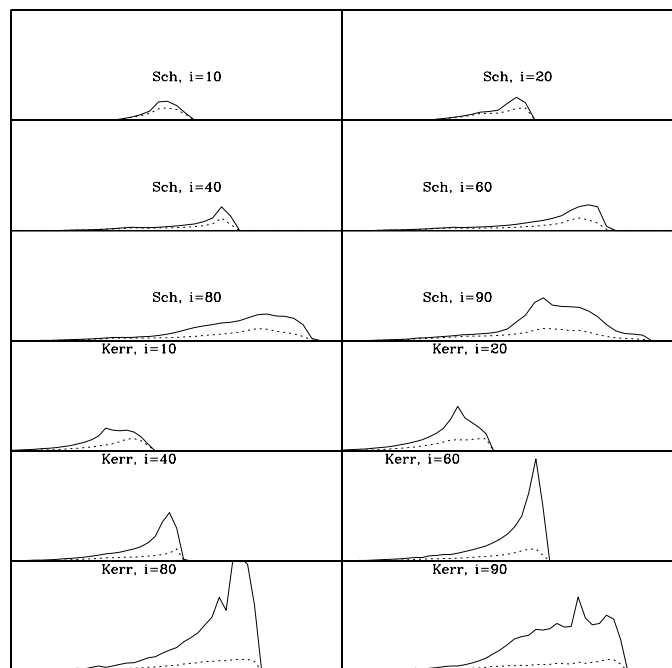


Fig. 3. Influence of inclination in the deformation of the Fe K line shape (dashed line) induced by MLE (solid line): $\text{REE} = 10 R_g$, $X_0 = -5$, $Y_0 = 5$, for the different inclination (i) of the disc in Schwarzschild (Sch) and Kerr (Kerr) metrics. The relative intensity is in the range from 0 to 10 (the maximum of unperturbed Fe K_α line is normalized to 1), and v/v_0 is from 0.4 to 1.8.

(1.0–1.2, - - -) parts of the line. As we can see the caustic crossing can produce significant amplification of the line flux. As in the case of the isolated microlens, the amplification is higher in the Kerr metric. This is in agreement with previous investigation by Jaroszyński et al. (1992) for continuum radiation of

the disc in the Schwarzschild and Kerr metrics. The line enhancement is also stronger in the blue part of the line, with this asymmetrical trend more marked in the Schwarzschild case.

4. Physical scenarios for the microlensing of the AGN Fe K_α line

In this section, we are going to explore two different physical scenarios in which microlensing could induce detectable changes in the line profile of the Fe K_α line.

4.1. Microlensing by a star-sized object in an intervening galaxy

In the standard configuration, microlensing affects one of the images of a lensed QSO and is produced by a star-sized object in the lens galaxy. An event of this type affecting the Fe K_α line has been reported in the quadruple imaged QSO J0414+0534 by Chartas et al. (2002). These authors observed a sudden increase in the iron line equivalent width from ~ 190 eV to 900 eV only on image B of J0414+0534 proposing that it has been caused by a microlensing event. We can try to reproduce this enhancement with our models under the assumption of amplification by a straight fold caustic crossing. However the problem is highly unconstrained because both sets of variables, the one related to the microlensing (relative amplification, β , orientation of the caustic with respect to the rotation axis, direction of the caustic crossing, microlens mass) and the one related to the relativistic disc model (outer radius, emissivity, metric) should be considered to fit a unique number. Thus, we can do only an exploration of scenarios compatible with the result. In first place we can fix the disc parameters adopted until now to study which values of the parameter β can reproduce the observed amplification in both metrics, Schwarzschild and Kerr. We have computed the maximum amplification for a caustic crossing along the X axis. The resulting amplifications, summarized in Table 1, indicate that there is a range of β values and microlens masses that can give rise to the observed amplification. For instance, for the value $\beta = 0.2$ (Chartas et al. 2002), a microlens of a solar mass can produce the observed enhancement. For $\beta = 1$, a low mass lens ($\sim 0.001 M_\odot$) can also produce the required amplification.

In second place we can fix the relative microlensing amplification to these values and try to fit the outer radii for several values of the emissivity in both metrics, Schwarzschild and Kerr. The results are included in Table 2. As it can be seen the results are relatively independent of the outer radii; the emissivity being the more relevant parameter.

Oshima et al. (2001) have also reported the presence of a strong ($EW \sim 960$ eV) emission Fe K_α line in the integrated spectra of the the lensed QSO H 1413+117. Oshima et al. (2001) interpret this results as produced by iron K_α emission arising from X-ray re-processing in the broad absorption line region flow. Alternatively, we can assume that the individual spectra of the components (not available) are different, and that the excess emission in the iron line arises only from one of the components, like in the case of J0414+0534. The red-shifts for the source (2.558; Kneib et al. 1998) and the lens (0.9) in

Table 1. The maximal amplification of the line flux for different caustic parameter β and masses of deflector (M_{ml}) for the case of MG J0414+0534 and H 1413+117. The calculation was performed for disc with the same characteristic as in the previous case, but for $R_{\text{out}} = 100 R_g$. The calculations were performed for: a) Schwarzschild and b) Kerr metric.

a) Schwarzschild metric			
$M_{\text{ml}} (M_\odot)$	$A_{\beta=0.2}$	$A_{\beta=0.5}$	$A_{\beta=1}$
0.001	1.44	2.10	3.21
0.01	1.78	2.95	4.91
0.1	2.38	4.46	7.92
1	3.47	7.16	13.33
b) Kerr metric			
$M_{\text{ml}} (M_\odot)$	$A_{\beta=0.2}$	$A_{\beta=0.5}$	$A_{\beta=1}$
0.001	1.53	2.33	3.95
0.01	1.94	3.36	5.73
0.1	2.67	5.19	9.37
1	3.98	8.45	15.91

Table 2. The maximal amplification of the line flux for different disc parameters R_{out} and q for the case of MG J0414+0534 and H 1413+117. The calculation was performed for caustic parameters: $\beta = 0.2$, $M_{\text{ml}} = 1 M_\odot$, $A_0 = 1$.

Schwarzschild metric				
q/R_{out}	20	50	100	500
0	4.3	3.0	2.4	1.6
-1	4.4	3.1	2.6	1.7
-2	4.8	3.6	3.0	2.8
-3	5.2	4.8	4.3	4.1
-5	7.4	6.8	6.6	6.5
Kerr metric				
q/R_{out}	20	50	100	500
0	4.4	3.0	2.5	1.6
-1	4.5	3.2	2.8	1.7
-2	5.6	3.8	3.4	2.9
-3	6.4	5.9	4.9	4.8
-5	9.2	8.7	7.7	6.8

H 1413+117 are so similar to the ones in J0414+0534 that we can use Tables 1 and 2 also for H 1413+117. The observed enhancement of one order of magnitude (Oshima et al. 2001) in this object could be explained by a $1 M_\odot$ if $\beta \sim 0.5$.

Regardless of the true nature of the two events reported in J0414+0534 and H 1413+117, our analysis show that objects in a foreground galaxy with even relatively small masses can bring strong changes in the line flux. This fact is indicating that changes in the Fe K_α line flux will be higher than in the UV and optical lines. Thus, the observation of the iron line in multi-imaged AGNs opens new possibilities to study the unresolved structure in QSOs and also the nature and distribution of compact objects in lens galaxies.

4.2. Microlensing by massive stars in the halo of an AGN

The size of the ERR projected on the source, η_0 increases with the distance between the source and the microlens. For this

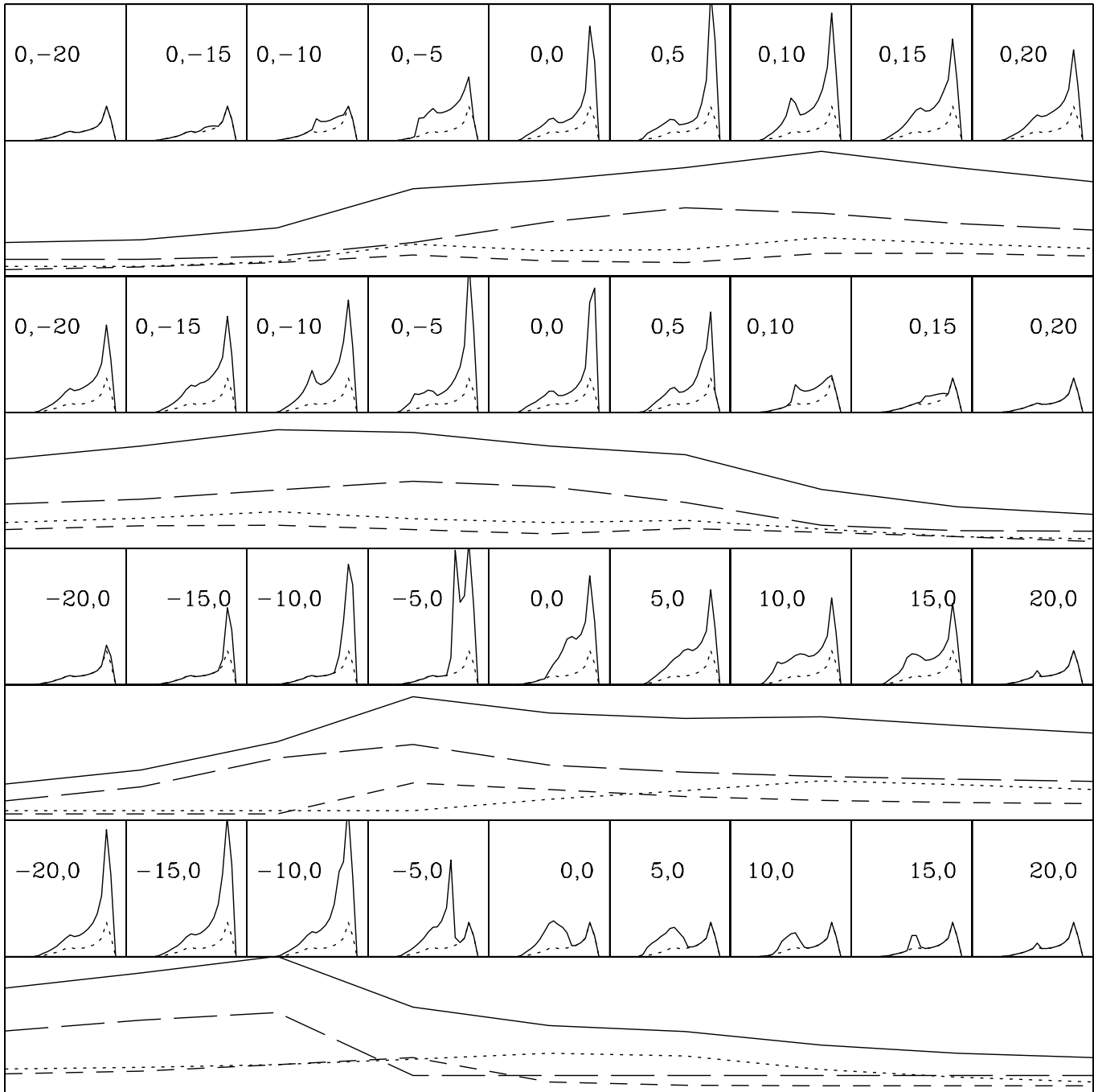


Fig. 4. The caustic crossing the disc with the same parameters as in Fig. 1. The first and second sequences of lines present the crossing of caustic perpendicular to the rotating axis for $\kappa = \pm 1$, respectively. The third and fourth sequences of lines present the caustic crossing along the rotation axis for $\kappa = \mp 1$, respectively. Below the sequences the corresponding line flux variation is presented: solid line presents the whole line flux variation, dashed lines present the variation of the red (0.4–0.9, - - -), central (0.9–1.0, - - -) and blue (1.0–1.2, — — —) parts of the line. The relative intensity ranges from 0 to 4 and v/v_0 ranges from 0.4 to 1.2. The parameters of the disc and caustic are given in the text.

reason, appreciable amplifications of the optical and UV BELs (i.e. η_0 comparable or greater than the dimensions of the accretion disc) induced by a star-sized object are only possible if the microlens is far away from the source, in an intervening galaxy (typically the lens galaxy). In the optical and UV case, appreciable amplifications of the BELs from an object in the host galaxy of the AGN are possible only by a very massive object (Popović et al. 2001a). However, due to the comparatively tiny

dimensions of the X-ray line emission region, microlensing of a star-sized object in the host galaxy becomes a possibility.

Since in the scenario we are considering, the distance, D , between the microlens and the accretion disc is negligible with respect to the distance between the observer and the microlens, the expression for η'_0 can be approximated as

$$\eta'_0 \approx \sqrt{\frac{4GM_{\text{ml}}}{c^2} \cdot D}, \quad (9)$$

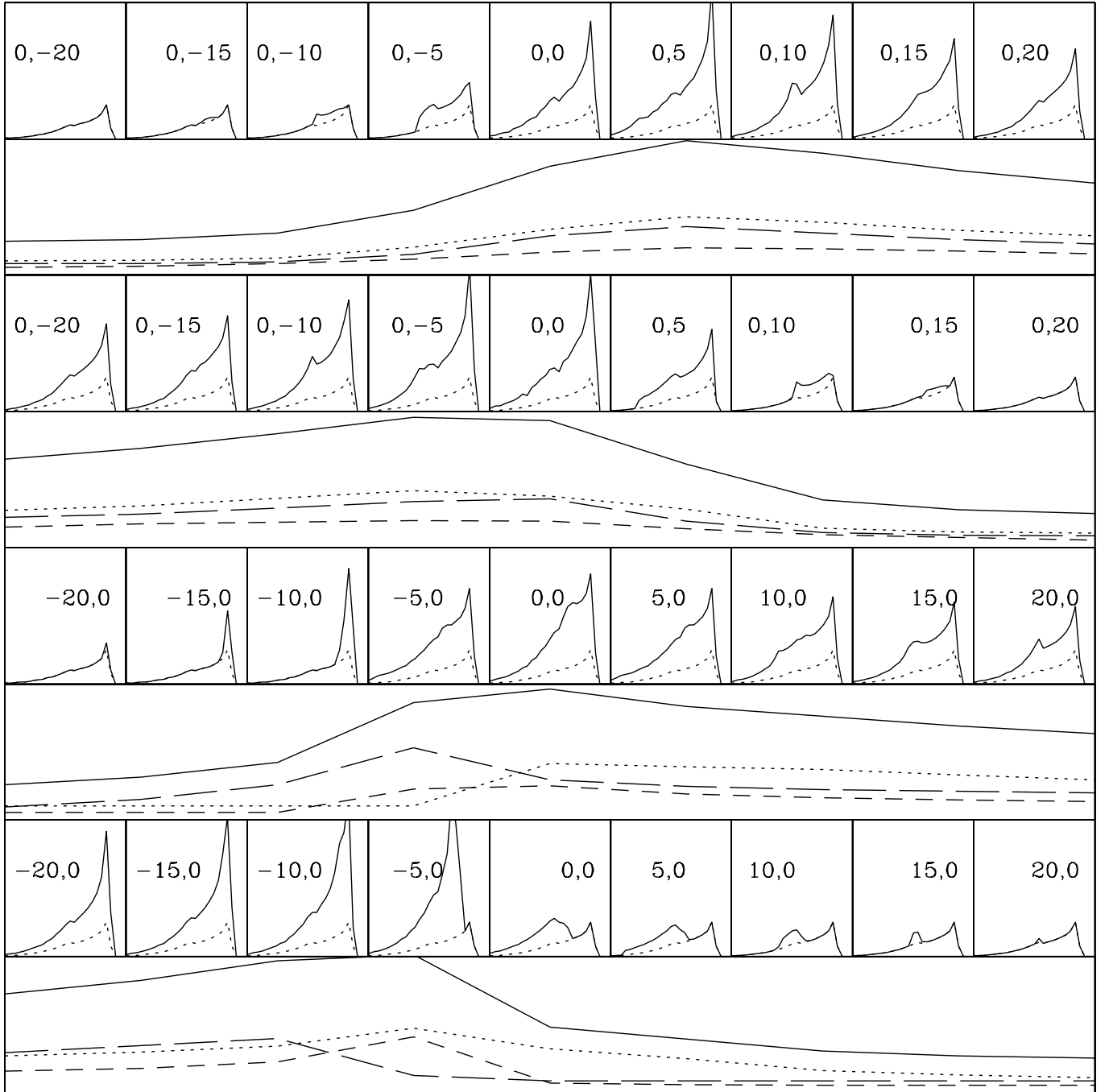


Fig. 5. The same as in Fig. 4 but for Kerr metric.

where $\eta'_0 = \eta_0 \cdot R_g$, and from Eq. (5) the mass of the microlens can be estimated as

$$M_{\text{ml}}[M_\odot] \approx \frac{\eta_0^2}{D} \cdot \frac{G}{4c^2} M_{\text{BH}}^2 = 1.19 \times 10^{-14} \cdot \frac{\eta_0^2}{D} M_{\text{BH}}^2, \quad (10)$$

where η_0 is given in gravitational radii, D is given in parsecs and M_{BH} is given in solar masses. Selecting distances between the accretion disc and the microlens in the interval 1 to 3 kpc (Schade et al. 2000), we obtain masses for the microlens which are smaller than solar in the case of BH with mass $\sim 10^7$, of the order of several solar masses for BH mass of $\sim 10^8$, and for a very massive black hole $\sim 10^9 M_\odot$ the microlens should have

significantly higher masses than solar. In Table 3 the estimation of microlens masses for a distance of 1kpc from the disc for three values of BH mass is given.

As one can see from Table 3, a low-mass deflector from the bulge of an AGN can produce significant changes in the line profile.

On the other side, the variation in the line profile and flux are very rapid in the Fe K_α line (see e.g. Vaughan & Edelson 2001). To estimate the time of microlens transition over the disc, we can use an approximative relation

$$\Delta t \approx \frac{D_{\text{disc}}}{V},$$

Table 3. The masses of the ML (in Solar masses) for different masses of BH, the assumed distance between deflector and the accretion disc is 1 kpc.

ERR in R_g	$M_{\text{BH}} = 10^7$	$M_{\text{BH}} = 10^8$	$M_{\text{BH}} = 10^9$
1	0.001	0.1	10
5	0.03	2.97	279
10	0.12	12	1200
20	0.48	48	4800
50	2.97	297	29 700

where D_{disc} is dimension of the disc, and V is velocity of microlens. As one can see from the Figs. 1–5, the part of disc where the influence is strong and can be noticeable is of the order of a few gravitational radii (or 10^{-6} – 10^{-4} pc, if we take that the velocity of microlens is of the order of $\sim 10^2$ km s^{-1} , we can estimate that the corresponding time of variation is of the order of 10^5 – 10^7 s.

The probability of seeing a MLE is usually expressed in terms of the optical depth τ . As far as the potential microdeflectors have an Einstein radius similar or larger than the radius of the disc, τ can be estimated as the fraction of the area in the source plane covered by the projected Einstein radii of the microlenses. Taking also into account that the distance between the accretion disc and the microlenses are negligible as compared with the distance between the observer and the microlenses

$$\tau \sim \frac{4\pi G}{c^2} \int_0^R \rho(r) r dr, \quad (11)$$

where R is the radius of the bulge or halo.

To estimate the order of magnitude of τ we assume a constant mass density, thus

$$\tau \approx \frac{2\pi G}{c^2} \rho_0 R^2. \quad (12)$$

Czerny et al. (2001) estimated that the total mass of the AGN bulges can reach values of $10^{12} M_\odot$ and Schade et al. (2000) found typical values for the radius of the AGN bulges in the range 1–10 Kpc. Both results yield a maximum optical depth from the bulge $\tau_b \sim 10^{-4}$. Using also favorable numbers for the galactic halo ($\rho \sim 0.01 M_\odot \text{ pc}^{-3}$, $R \sim 150$ Kpc) the optical depth could reach values of $\tau_h \sim 10^{-4}$. Adding both contributions a maximum optical depth $\tau \sim 0.001$ would be expected in a favorable situation. A detailed computation of τ , in addition to include accurate density profiles, should include a cut in the lower limit of integration (r_{min}) to exclude from the integral the microdeflectors with Einstein radii smaller than the radius of the disc (although the approximation $r_{\text{min}} \sim 0$ used does not change significantly the order of magnitude estimated for τ especially in the case of the halo).

In spite of the relatively low probability of microlensing by a deflector in the halo/bulge, we are going to explore the possibilities of detection in a practical case. We will study the case of NGC 3516. This galaxy was continuously monitored during 5 days by ASCA, and it was noted that the line flux does vary on a short time-scale (Nandra et al. 1999). We consider

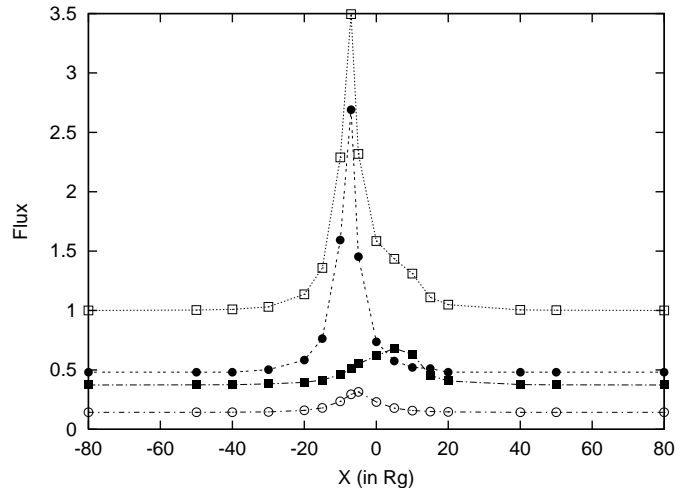


Fig. 6. The normalized flux variation in the central part (6.0–6.4 keV, open circles), blue wing (6.4–7.2, full circles), red part (2.0–6.0, full squares) and total line flux (open squares) as a function of position of the microlens. Calculation was performed for an accretion disc in Schwarzschild metric with parameters: $i = 35^\circ$, $R_{\text{inn}} = 60 R_g$, $R_{\text{out}} = 80 R_g$, and $q = 8$ (Nandra et al. 1999).

the Schwarzschild metric and a microlens with ERR of $10 R_g$ crossing along the disc (with $Y_0 = 0$).

The consequent variation of the flux of the Fe K_α line is presented in Fig. 6. The variation is higher in the blue wing, and even for the case of no such compact disc considered above ($80 R_g$), only a small (several R_g) region is responsible for the flux line variation, because the emission is very strongly concentrated in the inner disc. If we take that the BH mass is around 4×10^7 (Padovani et al. 1990), then we can estimate that the mass of a microlens with ERR = $10 R_g$ corresponds of $0.02 M_\odot$ at the distance of 1 kpc. As one can see from the figure such a small mass object can amplify the line emission by a factor 3 in a relatively short lapse of time (microlens crossing only several R_g). Moreover, the obtained results are in a good qualitative agreement with observations given by Nandra et al. (1999) where the line core seems to follow the continuum (very small changes in Fig. 6), while the blue wing is unrelated and shows a greater amplitude (~ 2). Moreover, the red wing presents very small variations, as in Nandra et al. (1999) observations.

5. Conclusions

In order to discuss the amplification and the shape distortion of the Fe K_α line, we have developed a ray-tracing model to study the influence of microlensing in a compact relativistic accretion disc. We consider both, the Schwarzschild and Kerr metrics. The main conclusions of our work are:

1) Microlenses of very small projected Einstein radii ($\sim 10 R_g$) can give rise to significant changes in the iron line profiles. The effects are two or three order of magnitude greater than the ones inferred for the UV and optical lines (Popović et al. 2001a). Off-centered microlenses would induce strong asymmetries in the observed line profiles.

2) The effects of microlensing show differences in the Kerr and Schwarzschild metrics, the amplitude of the magnification being greater in the Kerr metric. The transit of a microlens along the rotation axis of the accretion disc would induce a strong amplification of the blue peak in the Schwarzschild metric when the microlens was centered in the approaching part. In the Kerr metric the amplification will be greater but will not affect so preferentially the blue part of the line. This difference could be interesting to probe the rotation of an accretion disc.

3) Even objects of very small masses could produce observable microlensing in the iron K_α line of multiple imaged QSOs. We obtain that microlenses of 1 solar mass can explain the measured Fe K_α line excess in the J0414+0534 and H 1413+117 lens systems.

4) We have also found that stellar mass microlenses in the halo/bulge of the host galaxy could produce significant changes in the iron lines of an AGN. However, the optical depth is low, $\tau \sim 0.001$, even in favorable cases.

Acknowledgements. This work is a part of the project P6/88 “Relativistic and Theoretical Astrophysics” supported by the IAC and “Astrophysical Spectroscopy of Extragalactic Objects” supported by the Ministry of Science, Technologies and Development of Serbia.

References

- Abajas, C., Mediavilla, E. G., Muñoz, J. A., Popović, L. Č., & Oscoz, A. 2002, *ApJ*, 576, 640
- Bao, G., Hadrava, P., & Ostgaard, E. 1994, *ApJ*, 435, 55
- Bromley, B. C., Chen, K., & Miller, W. A. 1997, *ApJ*, 475, 57
- Čadež, A., Fanton, C., & Calivani, M. 1998, *New Astron.*, 3, 647
- Czerny, B., Nikolajuk, M., Piasecki, M., & Kuraszekiewicz, J. 2001, *MNRAS*, 325, 865
- Chang, K., & Refsdal, S. 1984, *A&A*, 132, 168
- Chartas, G., Agol, E., Eracleous, M., et al. 2002, *ApJ*, 568, 509
- Fabian, A. C., Iwashawa, K., Reynolds, C. S., & Young, A. J. 2000, *PASP*, 112, 1145
- Fanton, C., Calivani, M., Felice, F., & Čadež, A. 1997, *PASJ*, 49, 159
- Iwashawa, K., Fabian, A. C., Young, A. J., Inoue, H., & Matsumoto, C. 1999, *MNRAS*, 306, L19
- Jaroszyński, M., Wambsganss, J., & Paczyński, B. 1992, *ApJ*, 396, L65
- Kaspi, S., Smith, P. S., Netzer, H., et al. 2000, *A&A*, 333, 631
- Kneib, J. P., Allion, D., & Pelló, R. 1998, *A&A*, 339, L65
- Nandra, K., George, I. M., Mushotzky, R. F., Turner, T. J., & Yaqoob, T. 1997, *ApJ*, 477, 602
- Nandra, K., George, I. M., Mushotzky, R. F., Turner, T. J., & Yaqoob, T. 1999, *ApJ*, 523, L17
- Nemiroff, R. J. 1988, *ApJ*, 335, 593
- Narayan, R., & Bartelmann, M. 1999, in *Formation of Structure in the Universe*, ed. A. Dekler, & J. P. Ostriker (Cambridge University Press), 360
- Oshima, T., Mitsuda, K., Fujimoto, R., et al. 2001, *ApJ*, 563, L103
- Padovani, P., Burg, R., & Edelson, R. A. 1990, *ApJ*, 353, 438
- Popović, L. Č., Mediavilla, E. G., & Muñoz, J. 2001a, *A&A*, 378, 295
- Popović, L. Č., Mediavilla, E. G., Muñoz, J., Dimitrijević, M. S., & Jovanović, P. 2001b, *Serb. Aston. J.*, 164, 73 (Also, presented on GLITP Workshop on Gravitational Lens Monitoring, 4–6 June 2001, La Laguna, Tenerife, Spain)
- Schade, D. J., Boyle, B. J., & Letawsky, M. 2000, *MNRAS*, 315, 498
- Schneider, P., & Wambsganss, J. 1990, *A&A*, 237, 42
- Schneider, P., Ehlers, J., & Falco, E. E. 1992, *Gravitational Lenses* (Springer-Verlag, Berlin Heidelberg, New York)
- Vaughan, S., & Edelson, R. 2001, *ApJ*, 548, 694
- Wandel, A., Peterson, B. M., & Malkan, M. A. 1999, *ApJ*, 526, 579
- Witt, H. J., Kayser, R., & Refsdal, S. 1993, *A&A*, 268, 501